ISEIS

Journal of Environmental Informatics 40(1) 1-15 (2022)

Journal of Environmental Informatics

www.iseis.org/jei

Statistical Optimization of *Microcystis* Growth and Microcystin Production in Natural Phytoplankton Community Using Microcosm Bioassays

Z. Y. Wang[1, 2], P. F. Wang[1], C. Wang[1 *], S. H. Zhang[1], J. Hou[1], and Y. H. Ao[1]

[1] *Key Laboratory of Integrated Regulation and Resource Development on Shallow Lakes of Ministry of Education, College of Environment, Hohai University, Nanjing 210098, China*

[2] *Center for Eco-Environmental Research, Nanjing Hydrulic Research Institute, Nanjing 210029, China*

Received 28 August 2018; revised 7 April 2021; accepted 26 April 2021; published online 16 September 2021

ABSTRACT. Eutrophication of freshwater lakes and reservoirs causing toxic cyanobacterial blooms has become a global health concern. Commonly used approaches of statistical modelling have not fully captured the complex response of cyanobacterial biomass and microcystin concentration in response to stochastic variation of ambient conditions. This study applied statistically-based experimental design to screen out critical environmental factors, and to investigate the interactive effects of total nitrogen (TN), total phosphorus (TP), temperature (T) and light intensity (L) on *Microcystis* (MA) growth and microcystin (MC) production in the natural phytoplankton community. A batch of central composite designed nutrient enrichment bioassays (CCD-NEBs) were conducted in an ambient-controlled microcosm based on pneumatic annular flume system. Second-order polynomial CCD regression models predicting MA density and MC concentration were established and validated. MC concentration was found positively related to MA dominance. The interactive effects of TN-TP and TN-L on both MA density and MC concentration were determined to be more significant than other factors. Ranges of the optimum TN/TP ratio for MA growth and MC production under various environmental conditions were defined as 9.5 ~ 10.2 and 9.9 ~ 10.4, respectively. The ranges of nutrient thresholds for MA density of 2.00×10^4 cells mL^{-1} and MC concentration of 1.0 μg L^{-1} under different temperature and light conditions were evaluated, respectively. This study revealed that nutrient thresholds for MA blooming events and cyanotoxins safety guideline were fluctuant under lake-dependant conditions of temperature and light intensity, and the optimum TN/TP mass ratios should be alerted for the eutrophication management of blooming formation and microcystin safety.

Keywords: Microcystis, microcystin, pneumatic annular flume, response surface, nutrient threshold, nutrient enrichment bioassay

1. Introduction

Rapid and excessive cyanobacterial abundance usually forms massive blooms in eutrophic freshwater lakes and reservoirs, diminishing the water quality and leading to the scums, reduction of water clarity, and oxygen depletion (Donald et al., 2013). *Microcystis* (MA) is one of the most harmful bloom-forming cyanobacterium and its large-scale bloom has been reported as the visible symptom of accelerated eutrophication nearly from every continent (Otten et al., 2012; Bouhaddada et al., 2016; Steffen et al., 2017). The proliferation and sensecence of MA leads to the production and release of microcystins (MCs), destroying ecological balance and human health (Genuário et al., 2016).

MA growth is a complex activity based on a number of interior physical, chemical and biological mechanisms, and is potentially influenced by multiple exterior environmental factors. These include not only the abiotic factors such as nutrients (Elliott, 2014; Xu et al., 2015), temperature (Liu et al., 2011; Zhang et al., 2016), and light intensity (Torres et al., 2016), but also the biotic factors such as competition and grazing (Zhu et al., 2015). Since these environmental factors exist individually but present simultaneously, investigations on the interactive effects of such environmental factors on MA growth provide a better understanding on the formation of MA blooms at any choice of geographic location (Geada et al., 2017).

Although the independent influence of these factors on MA growth have been extensively studied in laboratory cultures and field investigations (Otten et al., 2012; Yu et al., 2014), few studies have identified how changes in the synergic effects of environmental variables contribute to the fluctuations in cyanobacteria populations. Jiang et al. (2008) applied response surface methodology (RSM) and established a central composite model to simulate the combined effect of nutrients, temperature, light intensity and iron on MA growth and MC content. Yang et al. (2012) evaluated the combined effect of temperature, light intensity, and nitrogen concentration on MA growth. Wang et al. (2016) studied the co-effects of nutrients, temperature, and light intensity on phytoplankton growth using RSM. These previous studies were conducted with isolated MA strains in the basic form of nutrient enrichment bioassays (NEBs) under static culturing conditions, while failure to account for the intraspecific and interspecific competition in phytoplankton

* Corresponding author. Tel.: +86 258-3786971; Fax: +86 258-3786971.
E-mail address: cwang@hhu.edu.cn (C. Wang).

ISSN: 1726-2135 print/1684-8799 online
 doi:10.3808/jei.202100455

succession might bias the estimates on MA biomass (Narwani et al., 2017). Further, productivity and community structure of phytoplankton are influenced by hydrologic disturbances in many ways (Buyukates and Roelke, 2005; Wang, 2015). The algal research performed in artificially static laboratory conditions might encourage growth of certain algal strains that required less energy exchange, likely missing important phenomena that are critical for understanding algal responses under real aquatic conditions (Lucker et al., 2014). To address these issues, it is meaningful to test the growth of MA strain in a lab-scale culture system capable of simulating both hydrodynamic environment present in natural water and fluctuating influential environmental factors.

MCs, known as the most ubiquitous cyanotoxin in freshwater ecosystems, is a family of cyclic heptapeptide toxins synthesized by a multi-functional protein complex in cyanobacterial cells and released through cell wall (Daly et al., 2007). Strains of several cyanobacterial genera can synthesize MCs, including Microcystis, Anabaena and Planktothrix (Dolman et al., 2012). Hence, increases in biomass of dominant MC-producing cyanobacterial taxa are typically associated with elevated concentration of MCs (Monchamp et al., 2014). Toxin-producing MA may present higher tolerance to environmental change and gain a competitive advantage over other algae, thus becoming superior competitors in phytoplankton community (Huang et al., 2012). Some previous studies have extensively discussed the effect of single environmental factors on the abundance of toxin-producing MA and synthesis of cyanotoxins (Domingues et al., 2012; Pimentel and Giani, 2014; Wei et al., 2016). The co-effects of temperature, light intensity, nitrate and phosphate on the dominance of MC-producing MA strains were examined in monoculture and co-culture experiments (Lei et al., 2015). However, to our knowledge, the commonly used approaches of statistical modeling have not fully captured the complex response of toxic MA biomass and MC concentration in relation to the stochastic variation of ambient conditions, limiting our ability to predict and mitigate the impairment of freshwaters by toxic algal blooms.

RSM is commonly used for multi-variable experimental design, value prediction, and estimation of synergistic effects among sequentially involving factors with a limited number of experiments. Instead of allowing to understand the internal mechanism of the system or process, RSM tends to find a suitable approximating function for the purpose of predicting the future response and determining the optimum operating conditions where the certain operating specifications are met. It has proved to be a more efficient statistical approach than the complicated and time-consuming one-factor-at-a-time method (Kong et al., 2014). Several RSM attempts have successfully identified the interactions among a large number of processing variables and evaluated the heterogeneous responses (Hanrahan, 2007; Beuckels et al., 2015). The application of statistical experimental design techniques in algal prediction could result in reduced process variability and closer confirmation of output response to nominal requirements (Wang et al., 2016; Wang et al., 2017).

In this study, we performed a batch of statistically designed nutrient enrichment bioassays (NEBs) in a patented ambient-controlled microcosm system, which was designed to replicate the real hydrodynamic environment that impact algal physiology, energy capture, and life cycle. The response surface models were established to screen critical environmental factors and predict their combined effects on MA growth and MC production in the natural phytoplankton community. Our study predicts the dynamic nutrient thresholds for MA blooming events and cyanotoxins safety guideline under lake-dependant conditions of temperature and light intensity, as well as the optimum TN/TP mass ratios for MA growth and MC production. The theoretical framework presented herein aspires to advance our understanding of global emergent drivers of MA-dominant blooms as well as management strategies for cyanotoxin control.

2. Materials and Methods

2.1. Plackett-Burman Design for Factor Screening

To determine the variables which have significant effects on Microcystis growth and microcystin production, the potential environmental factors (pH, nitrogen, phosphorus, dissolved oxygen, velocity, turbidity, algal density, Microcystis dominance, temperature, light intensity) were screened in the first step by using Plackett-Burman (PB) design, as described by Jiang et al. (2008). Each variable was selected at the high level (+1) and low level (–1) (shown in Table S1). The low level (–1) of each variable was set at the point close to the concentration reported in the natural aquatic environment of Changtan Reservoir where the algal cultures were sampled (as described in Text S1 and Table S2). The high level (+1) of each variable was set much far higher from the low level (–1) to observe the significant effect if it existed. The PB design matrix was shown in Table S3. The MA density and MC content were estimated as the model responses, respectively. Effect of measured and corrected responses of each factor was calculated as follows:

$$E_X = \frac{\sum X(+)}{N/2} - \frac{\sum Y(-)}{N/2} \quad (1)$$

where X was real factors (A, B, C, …), E_X was the effect of X on response Y, $Y(+)$ and $Y(-)$ were the sums of responses at the highest and lowest levels of X, N was the number of the experimental runs in the PB design.

A total of 12 experimental combinations was designed for PB screening experiments. The statistical analytic results including effect, t-value and p-level were listed in Table S4. The factors that had significant effects on MA growth and MC production were screened out from PB design. It could be seen that four variables (nitrogen, phosphorus, temperature and light intensity) had significant effects on MA density ($p < 0.05$), while three variables (nitrogen, phosphorus, and light intensity) affected MC content significantly. The interactive effects of these significant factors were determined by the subsequent CCD design.

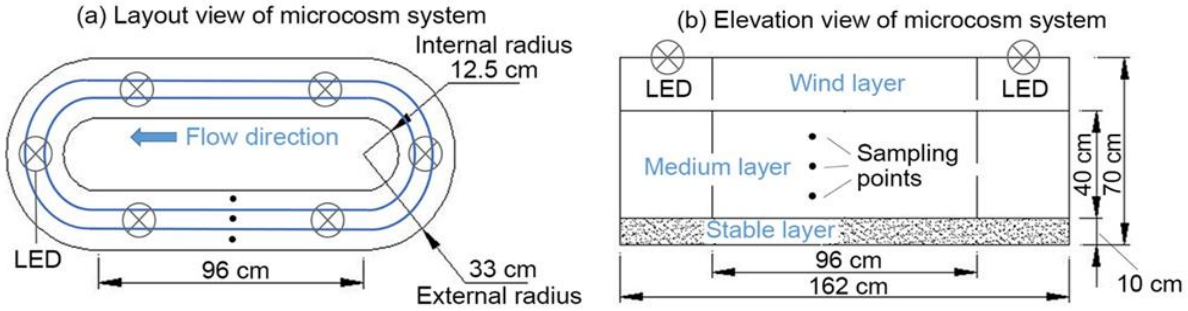

Figure 1. Schema of pneumatic annular flume microcosm system for central composite designed nutrient enrichment bioassays. (a) The microcosm system is designed to simulate the phytoplankton succession in circulated medium. The annular flume was divided into three orbits for experimental triplicates. The external and internal radius were 33 and 12.5 cm, respectively. The microcosm system was installed in a thermostatic chamber and exposed to photosynthetically active radiation provided by adjustable full-spectrum light emitting diode (LED) arrays designed for plant growth with spectral width of 360 ~ 780 nm; (b) The total length and height of the annular flume are 162 and 70 cm, respectively. Wind was provided by a blast blower and wind speed was adjusted to 3 m/s by modulation of ventilator angle and opening extent of a valve. A 10-cm-high stable layer and the 40-cm-high overlying nutrient medium were successively tapped into the annular flume. Identical water turbulence was induced in three orbits of the annular flume with mean flow velocities of surface water of 0.04 m/s.

2.2. Central Composite Design for NEBs

The experimental design of NEBs was based on the central composite design (CCD) derived from RSM. The basic CCD model settings referred to our previous work (Wang et al., 2017). The ranges of real values for each environmental factor in the CCD experimental design were defined as (a) total nitrogen (TN) of 0.2 ~ 2 mg L^{-1}; (b) total phosphorus (TP) of 0.02 ~ 0.2 mg L^{-1}; (c) temperature (T) of 18 ~ 34 °C; and (d) light intensity (L) of 28 ~ 142 μE m^{-2} s^{-1}. The selected ranges of these environmental factors for CCD design covered TN concentration, TP concentration, T and L reported in natural aquatic environments of Changtan Reservoir (Table S2). Each independent parameter varied over 5 coded levels ($-\alpha$, –1, 0, +1, $+\alpha$; α = 2 for rotatable designs in this study), which composed the CCD matrix with a total of 30 experimental runs (Table 1). As shown in Figure S1, the design matrix has 3 groups of design points, namely fractional factorial design points (coded as run 1 ~ 8 and run 23 ~ 30), axial points (coded as run 9 ~ 12 and run 19 ~ 22), and center points (coded as run 13 ~ 18). Run 13 ~ 18 served as the repetition of center points to get a desirable estimate of experimental error. MA density and MC concentration were estimated as model responses, respectively.

The true value of each variable X_i was coded as follows:

$$x_i = \frac{X_i - X_{ci}}{\Delta X_i} \quad (2)$$

where x_i was the coded level, X_i was the real value of an independent variable, X_{ci} was the real value of an independent variable at the central point, and ΔX_i was the step change of variable i.

The CCD model represented the independent environmental parameters as processing variables in a quantitative form:

$$Y = f(A, B, C, D) \quad (3)$$

where Y was the predicted responses (MA density and MC concentration in this study), A, B, C, and D were the coded levels of the actual variables (TN, TP, T, and L in this study).

The response values were first approximated by a suitble lower order polynomial in a linear manner, then the quaratic, cubic, and higher order polynomial. In our system with curvatures, a second-order polynomial in the form of a quaratic model was suggested as follows:

$$Y = k_0 + k_1A + k_2B + k_3C + k_4D + k_{12}AB + k_{13}AC + k_{14}AD + k_{23}BC + k_{24}BD + k_{34}CD + k_{11}A^2 + k_{22}B^2 + k_{33}C^2 + k_{44}D^2 \quad (4)$$

where k was the estimated coefficient of the equation.

The calculation of 15 coefficients in the above second-order polynomial equation derived from the standard CCD model established by Design Expert® (DX) 8.0 (Stat-Ease Inc., Minneapolis, MN, USA). By plotting the predicted responses according to the final quadratic polynomial equation in terms of coded factors, CCD model provided a rotatable 3D response surface plot and a corresponding contour plot to visualize the interactive effects of controlling parameters on the variation pattern of experimental data.

Graphical optimization of response surface plots was conducted on the basis of the desirability function with DX analysis to determine the optimal condition that minimizes or maximizes the corresponding responses, as described by Garg and Joshi (2017). The identification of nutrient thresholds was based on a consistent set of overlaying contour graphs highlighting an area of operability for desirable responses. By digitizing the contour curves and coordinating unique curve points with DX analysis, border values of TN and TP in the corresponding operating area for the specific criteria of model response were identified as nutrient thresholds.

Table 1. CCD Experimental Matrix of Four Environmental Variables in Five Coded Levels

Level	TN (mg L^{-1})		TP (mg L^{-1})	T (°C)	L (μE m^{-2} s^{-1})
+2	2.000		0.200	34	142
+1	1.550		0.155	30	113
0	1.100		0.110	26	85
−1	0.650		0.065	22	57
−2	0.200		0.020	18	28
Run	Coded variables				MA density*	MC concentration*
	TN	TP	T	L	(10^4 cells mL^{-1})	(μg L^{-1})
1	−1	−1	−1	−1	1.21 ± 0.56	7.5 ± 0.2
2	+1	−1	−1	−1	0.50 ± 0.02	3.3 ± 0.2
3	−1	+1	−1	−1	1.05 ± 0.05	5.9 ± 0.5
4	+1	+1	−1	−1	1.25 ± 1.01	8.6 ± 0.6
5	−1	−1	+1	−1	1.93 ± 0.72	10.7 ± 1.5
6	+1	−1	+1	−1	0.57 ± 0.20	3.6 ± 2.0
7	−1	+1	+1	−1	0.45 ± 0.04	2.5 ± 0.7
8	+1	+1	+1	−1	2.17 ± 0.53	11.3 ± 1.1
9	0	0	0	−2	1.29 ± 0.11	9.1 ± 0.4
10	0	0	−2	0	1.40 ± 0.72	9.0 ± 0.9
11	0	−2	0	0	0.25 ± 0.21	1.1 ± 3.0
12	−2	0	0	0	0.34 ± 0.11	1.6 ± 2.1
13	0	0	0	0	1.50 ± 0.18	9.7 ± 0.6
14	0	0	0	0	1.91 ± 0.09	10.6 ± 1.2
15	0	0	0	0	1.42 ± 1.13	8.8 ± 2.0
16	0	0	0	0	1.40 ± 0.25	8.7 ± 1.6
17	0	0	0	0	1.43 ± 0.66	9.0 ± 0.2
18	0	0	0	0	1.55 ± 0.72	9.2 ± 0.2
19	+2	0	0	0	0.75 ± 0.34	4.2 ± 0.7
20	0	+2	0	0	1.17 ± 0.82	6.3 ± 5.7
21	0	0	+2	0	1.75 ± 0.15	10.1 ± 1.4
22	0	0	0	+2	2.25 ± 1.03	12.6 ± 5.2
23	−1	−1	−1	+1	1.06 ± 0.43	5.8 ± 0.1
24	+1	−1	−1	+1	1.19 ± 0.28	8.2 ± 0.5
25	−1	+1	−1	+1	1.02 ± 0.10	5.2 ± 0.5
26	+1	+1	−1	+1	2.35 ± 0.58	13.5 ± 0.5
27	−1	−1	+1	+1	1.17 ± 1.02	7.8 ± 1.7
28	+1	−1	+1	+1	0.94 ± 0.75	5.4 ± 0.1
29	−1	+1	+1	+1	1.08 ± 0.77	6.3 ± 2.1
30	+1	+1	+1	+1	2.42 ± 0.91	15.6 ± 0.6

* expressed as mean value ± standard deviation

2.3. Experimental Procedure of NEBs

The batch of CCD-NEBs were performed in a pneumatic annular flume (PAF) microcosm system (Patent No. 2007100-25671.3, Hohai University, China), which was designed to simulate the phytoplankton succession in circulated medium. The microcosm system consists of an annular flume with a total height of 0.7 m and a wind blast blower (Figure 1). The annular flume was divided into three orbits for experimental triplicates. The main driving force of water turbulence in this pneumatic annular flume microcosm system was wind, and the surface wind induced an energetic wave-affected current enhancing the flow velocity of surface water significantly. By using a thermal anemometer and an acoustic Doppler velocimeter, we measured wind speeds and flow velocity at the sampling points in the pneumatic annular flume microcosm system when the flow structure reached a stable profile. A 60 s data were sampled at the frequency of 50 Hz from bottom to water surface with 1 cm step under wind forcing at each sampling position at the perpendicular bisector of cross-section. By modulation of ventilator angle and opening extent of a valve, the wind speed was adjusted to 3 m/s which induced water turbulence with mean flow velocities of surface water of 0.04 m/s in three orbits of the annular flume. At the wind speed of 3 m/s, the vertical distributions of longitudinal velocity component in three orbits did not exhibit significant difference. The experimental configuration referred to the protocol described in our previous work

(Zheng et al., 2013). The overlying nutrient medium with thickness of 0.4 m were tapped into the PAF system and ran for at least 2 h to reach a stable profile of water flow. To maintain a desirable ambient temperature and light intensity, the microcosm system was installed in a thermostatic chamber and exposed to photosynthetically active radiation provided by adjustable full-spectrum light emitting diode (LED) arrays designed for plant growth with spectral width of 360 ~ 780 nm.

The natural algal samples for NEBs were collected with a plankton net (30 μm pore size, Pogson™ PT-25, China) from the blooming area of eutrophicated Changtan Reservoir in Guangdong Province, China (detailed in Text S1). All samples were sealed in sterile polyethylene bottles and kept in cooler box until transferred to the laboratory within 4 hrs. The algal samples collected from Changtan Reservoir were centrifuged to suspensions at a speed of 15,000 rpm for 10 min, and algal cells were then separated from water and maintained as algal cultures. To eliminate bacterial contamination, these algal cultures were sequentially subjected to a repeated washing, lysozyme/SDS, and antibiotic mixture treatment according to the protocol described by Su et al. (2007). Epifluorescence microscopic examination was conducted to verify that no bacterial impurities existed in the treated algal cultures. To exclude the possibility that lysozyme or SDS lysed algal cells, the integrity of algal cells was identified and compared with the controls by microscopic examination after these treatments. To detect the possible existence of in-vivo bacteria, 10 mL aliquots of the treated algal samples were subcultured three times in sterile BG11 medium to verify the absence of potential bacterial contamination.

The axenic algal cultures were then starved in sterile BG11 medium with N and P excluded under 25.0 ± 0.5 °C with an illumination intensity of 40 μE m^{-2} s^{-1} and a light/dark photoperiod of 12/12 h. The composition of BG11 culture medium was shown in Table S5. The containers were autoclaved (MLS-37-50, Sanyo™, Japan) at 120 °C and 1.2 atm for 2 h as aseptic techniques. After a 2-week incubation, algal cells were harvested by centrifugation (4,000 rpm, 4 °C, 5 min) and diluted with fresh BG11 medium to reach a desirable initial density of 750 ± 56 cells mL^{-1} after inoculation in the microcosm system. The community composition of the algal culture used for NEBs was described in Table S6.

In CCD-NEBs, the algal cultures were grown in modified BG11 medium with controlled N and P levels at a gradient of designated temperature and light intensity with a light/dark photoperiod of 12/12 hr. The analytical reagents sodium nitrate ($NaNO_3$, > 99% purity) and potassium phosphate dibasic (K_2HPO_4, > 99% purity) were used as N and P sources. Stock solutions of 1 mg L^{-1} for both nutrients were prepared by dissolving $NaNO_3$ and K_2HPO_4 in Milli-Q deionized water (Millipore™ water purification system, Bedford, MA, USA). Appropriate aliquots of the stock solutions were daily replenished into the microcosm system to obtain the designated nutrient levels of CCD designed experimental runs (Table 1). Based on previous documentation (Domingues et al., 2011; Huang et al., 2012) and our preliminary experimental results, the experimental period of NEBs in our study was set to 7 days.

2.4. Analysis of Phytoplankton Community and MC Concentration

Five milliliters of algal culture broth were sampled aseptically and centrifuged at 4,000 rpm for 5 min. The cell enumeration at the species level was performed by observing hemacytometer counting chambers under a standard compound (upright) microscope (Carl Zeiss™ Light Microscopy, Axioskop 40 Pol, Germany) at 400× ~ 1000× magnification. The algal cell numbers were converted to algal density expressed as cell number per milliliter. The phytoplankton species were identified according to Hu's standard protocol (2006).

Fifty milliliters of algal culture broth was collected and freeze-dried for MC concentration analysis. The freeze-dried sample was dissolved in 5% acetic acid solution and sonicated for 30 min with an ultrasonic disruptor (KQ3200DE, Shumei®, China). The completely lyophilized cells were dispersed in deionized water and subjected to three freeze/thawing cycles at –70 °C in liquid nitrogen prior to centrifuge separation at 6,000 rpm at 4 °C for 15 min. The supernatant was collected for total MC concentration analysis with a direct competitive Enzyme-Linked Immunosorbent Assay (ELISA) kit (Quantiplate™, Envirologix, ME, USA) using a polyclonal antibody bound to a microtiter plate.

MC-LR standard (98% purity) was purchased from A.G. Scientific (San Diego, CA, USA) and all measurements were expressed in MC-LR equivalents. The positive control, negative control, fortified sample, and duplicate sample were run for every 10 samples. Recovery of MC-LR standard addition fell within the limits of 95.9 ~ 103.2%. The correlation coefficient was > 0.999 and the limit of detection was 50 ng L^{-1}. Each sample was analyzed in triplicate and samples with coefficient of variation higher than 15% were reanalyzed, following the protocols recommended by the manufacturer.

2.5. Statistical Analysis Methods

The data were subjected to lack-of-fit test based on analysis of variance (ANOVA) to evaluate the accuracy and applicability of response surface model. The statistical significance of independent variables and their interactions (combinations of two codes) at various levels of probability were checked by Student's *t*-test and *p*-values. Variables with high levels of significance were associated with high values of parameter estimates to indicate their importance in the variation of responses. The statistic *F*-value, coefficient of variation, and adjusted coefficient of determination were calculated. The lack of fit contained in the residuals was checked by the normal probability plot and parity plot of residuals. The model precision was elucidated by the signal-to-noise ratio, which compared the range of predicted values at the design points to the average prediction error.

The data were respectively checked by the Kolmogorov-Smirnov one-sample test and Levene's test to determine the normality and the homogeneity of variance. If both of the assumptions agreed, a one-way ANOVA followed by Tukey's multiple comparison tests were employed to assess the differ-

ences among treatments. Parameters that did not meet both of these assumptions were subjected to a log-transformation before ANOVA. Significance values were assumed at $p < 0.05$. The statistical analysis was performed using OriginPro 8.5 (OriginLab Corporation, Northampton, MA, USA) and SPSS 17.0 (SPSS Inc., Chicago, IL, USA).

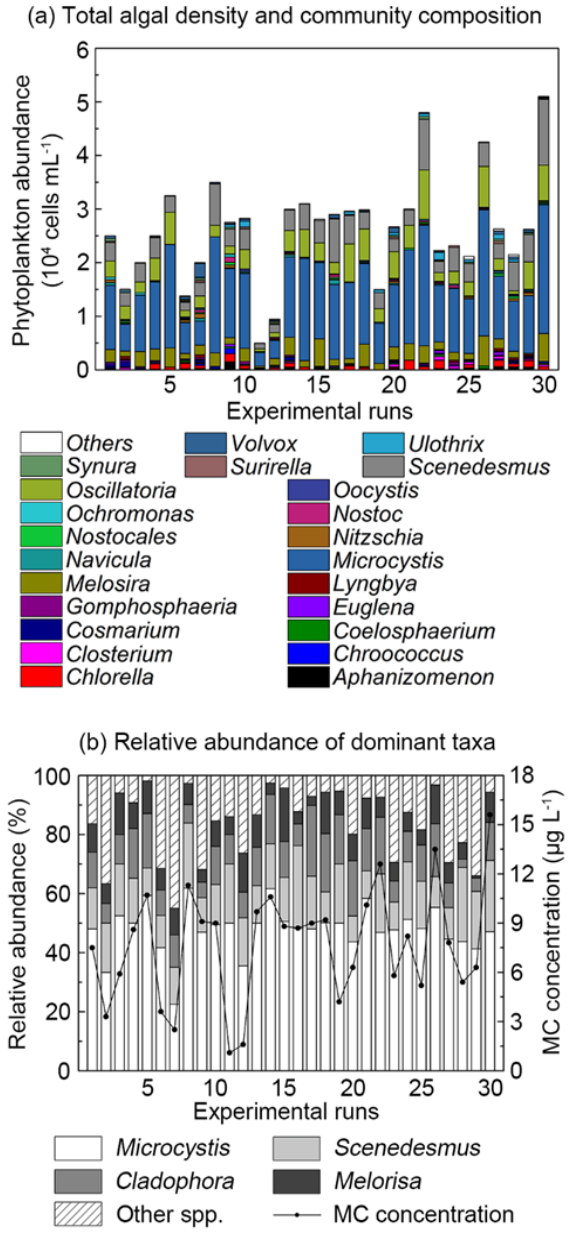

Figure 2. Variation of phytoplankton community under different experimental conditions in nutrient enrichment bioassays. (a) Total algal density and phytoplankton community composition in different experimental runs; (b) Relative abundance of dominant algal taxa and microcystin content measured in different experimental runs. The dominant algal taxa are *Microcystis*, *Scenedesmus*, *Cladophora*, and *Melorisa*.

3. Results

3.1. Variation of Phytoplankton Community in Different Groups of NEBs

A total of 81 species among 5 phytoplankton phyla were identified in the batch of NEBs (listed in Table S7). The variation of phytoplankton community under different experimental conditions in NEBs is shown in Figure 2(a). The 25 observed phytoplankton genera included Charophyta (*Closterium* and *Cosmarium*), Chlorophyta (*Chlorella*, *Cladophora*, *Oocystis*, *Scenedesmus*, *Ulothrix*, and *Volvox*), Cyanobacteria (*Anabaena*, *Aphanizomenon*, *Chroococcus*, *Coelosphaerium*, *Gomphosphaeria*, *Lyngbya*, *Microcystis*, *Nostoc*, and *Oscillatoria*), Euglenozoa (*Euglena*) and Ochrophyta (*Melosira*, *Navicula*, *Nitzschia*, *Ochromonas*, *Pediastrum*, *Surirella*, and *Synura*). As shown in Figure 2(b), the relative abundance of MA was higher than 50% in most runs of the NEBs. Scenedesmus, Melosira, and Oscillatoria with relatively high proportion were identified as the second-dominant genera. MA dominance and MC content showed a significant positive correlation ($r = 0.601$, $p < 0.05$).

3.2. CCD Response Surface Modeling for MA Density and MC Concentration

The CCD response surface models simulating the interactive effects of significant environmental parameters on MA growth and MC production were accordingly established. The estimates of coefficients and the associated significant levels for the parameters in the second-order polynomial CCD models are shown in Table 2. The combination of two codes indicated an interaction effect between the two parameters. The first order (*A*, *B*, *D*), second order (A^2, B^2) and interactive (*AB*, *AD*) parameters exhibited a relatively significant influence ($p < 0.05$) on the variation of responses, while the other parameters were statistically insignificant. The coefficient estimation indicated that the first-order effects of all four environmental parameters were positive, while the second-order effects of TN and TP were negative. TN, TP, L, and their interactions were the most significant variables for the variation of responses.

By fitting the parameter coefficients estimated by CCD model, the second-order regression equations in terms of coded parameters were established to describe the responses of MA density (Y_{MA}) and MC concentration (Y_{MC}):

$$\begin{aligned} Y_{MA} = {} & 1.53 + 0.13[TN] + 0.21[TP] + 0.075[T] + 0.17[L] \\ & + 0.42[TN][TP] + 0.031[TN][T] + 0.17[TN][L] \\ & - 0.015[TP][T] + 0.11[TP][L] - 0.072[T][L] - 0.23[TN]^2 \\ & - 0.18[TP]^2 + 0.033[T]^2 + 0.082[L]^2 \end{aligned} \quad (5)$$

$$\begin{aligned} Y_{MC} = {} & 9.33 + 0.65[TN] + 1.30[TP] + 0.28[T] + 0.87[L] \\ & + 2.53[TN][TP] - 0.037[TN][T] + 1.09[TN][L] \\ & - 0.012[TP][T] + 0.64[TP][L] - 0.025[T][L] - 1.47[TN]^2 \\ & - 1.27[TP]^2 + 0.19[T]^2 + 0.52[L]^2 \end{aligned} \quad (6)$$

Table 2. The Estimated Coefficient and Statistical Significance of Coded Parameters in CCD Response Surface Models

Variables	Model for MA density		Model for MC concentration	
	p-value	Coefficient	*p*-value	Coefficient
Intercept		1.530		9.33
A - TN	0.0324*	0.130	0.0056*	0.65
B - TP	0.0023*	0.210	0.0074*	1.30
C - T	0.2110	0.075	0.4566	0.28
D - L	0.0103*	0.170	0.0406*	0.87
AB	< 0.0001*	0.420	< 0.0001*	2.53
AC	0.6676	0.031	0.8835	–0.037
AD	0.0299*	0.170	0.0031*	1.09
BC	0.8330	–0.015	0.9610	–0.012
BD	0.1336	0.110	0.1016	0.64
CD	0.3202	–0.072	0.9222	–0.025
A^2	0.0008*	–0.230	0.0001*	–1.47
B^2	0.0036*	–0.180	0.0003*	–1.27
C^2	0.5478	0.033	0.3431	0.19
D^2	0.1473	0.082	0.0829	0.52

* $p < 0.05$, significant model term

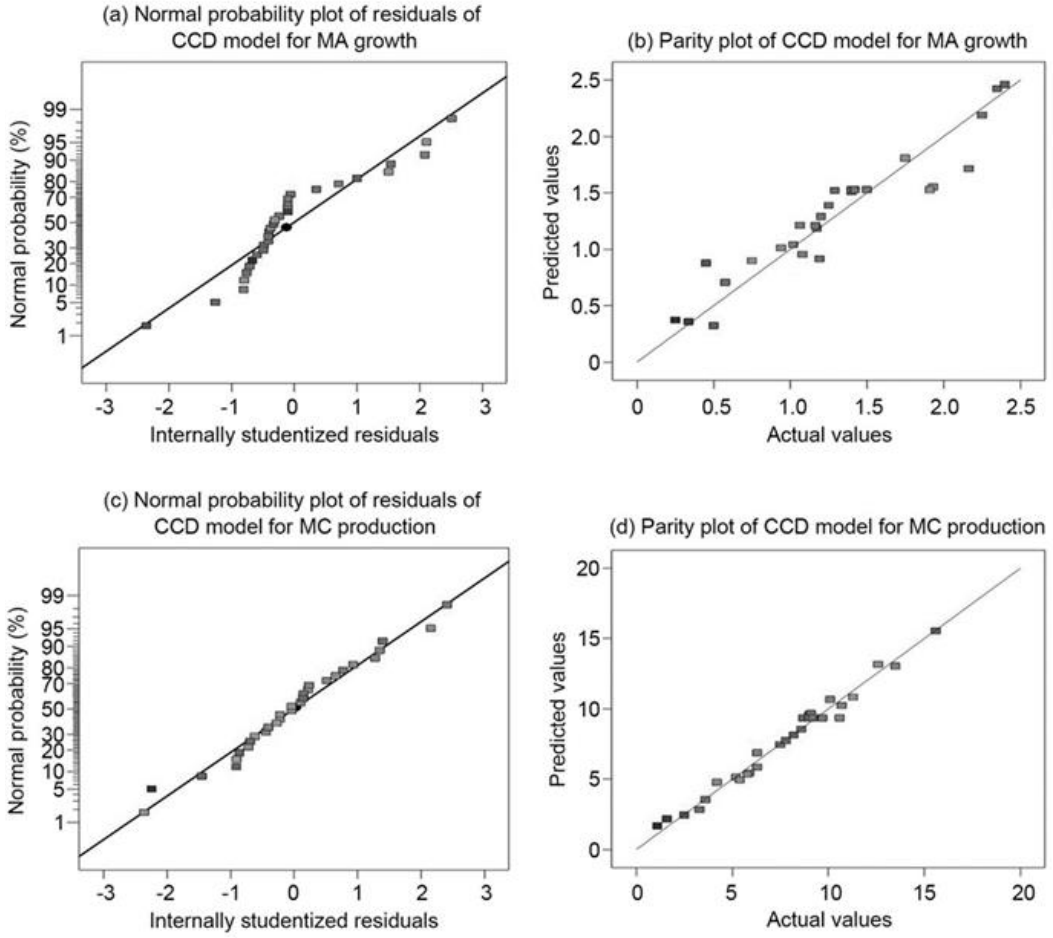

Figure 3. The normal probability plot of residuals and parity plot showing the correlation between the predicted and experimental values of CCD model for MA growth and MC production. (a) Normal probability plot of residuals of CCD model for MA growth; (b) Parity plot of CCD model for MA growth; (c) Normal probability plot of residuals of CCD model for MC production; (d) Parity plot of CCD model for MC production.

Table 3. Analysis of Variance (ANOVA) of CCD Response Surface Models

Sources of variation	Model of MA density	Model of MC concentration
Model		
F-value	7.80	15.99
p-value > *F*	0.0002	0.0005
Residual		
Lack of Fit	0.1483	0.0857
Pure Error	0.19	2.55
RMSE	0.28	0.99
Mean	1.29	7.71
C.V. (%)	21.69	12.81
R-squared	0.8793	0.9805
Adjusted *R*-squared	0.7666	0.9192
Adequate Precision	10.82	16.05

The low probability value ($p < 0.05$) and high Fisher *F*-test value showed that the CCD regression models were significant (Table 3). The lack of fit was not significantly relative to the pure error ($p > 0.05$). The goodness of regression was verified by the low root-mean-square error and high coefficients of *R*-squared. The relatively high values of model precision indicated a satisfactory model discrimination and an authentic relationship between the model responses and significant variables. The normal probability plot of residuals confirmed the assumptions that errors were normally distributed and error variances were homogeneous (Figures 3(a) and 3(c)). Points clustering around the diagonal line in the parity plot showed that no serious deviation between observed and predicted values was indicated (Figures 3(b) and 3(d)).

3.3. Interactive Effects of Environmental Factors on MA Growth

The 3D saddle-like response surface plot of MA density in function of TN and TP with a light intensity of 139 μE m^{-2} s^{-1} at 31.8 °C (average environmental condition of Changtan Reservoir in summer) is shown in Figure 4(a). Increasing TN and TP concentration facilitated the increase in MA density from 0.51×10^4 to 2.12×10^4 cells mL^{-1}, revealing the synergic promoting effect of nutrients. As shown in contour plot, the minimum response was obtained at the coded level of –2 for both TN and TP. The maximum response could be reached at the +2 levels of TN and TP. By conducting graphical optimization of response surface plots via DX analysis, the optimal TN/TP mass ratio that maximizes MA growth ranged between 9.5 and 10.2. The thresholds of TN and TP concentration that supported the minimum response for MA density at 2.00×10^4 cells mL^{-1} (the potential criterion of MA blooming event) ranged between 0.20 ~ 0.89 mg L^{-1} and 0.02 ~ 0.08 mg L^{-1} under different temperature and light conditions, respectively.

Figure 4(b) displays the response surface plot as a function of TN and light intensity on MA growth. As TN concentration increased, the stimulating effect of light intensity on MA growth was strengthened. The same variation pattern was observed as light intensity increased, where MA growth was more radically promoted with a higher level of TN concentration. It was noti-

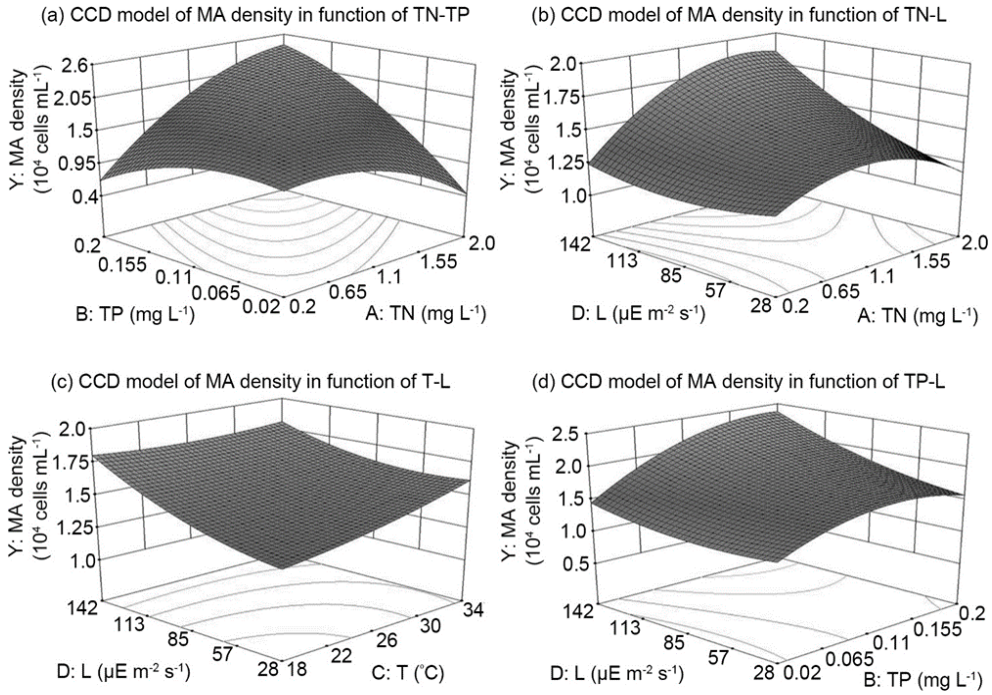

Figure 4. Response surface plots of CCD model of MA density. (a) CCD model of MA density in function of TN-TP; (b) CCD model of MA density in function of TN-L; (c) CCD model of MA density in function of T-L; (d) CCD model of MA density in function of TP-L.

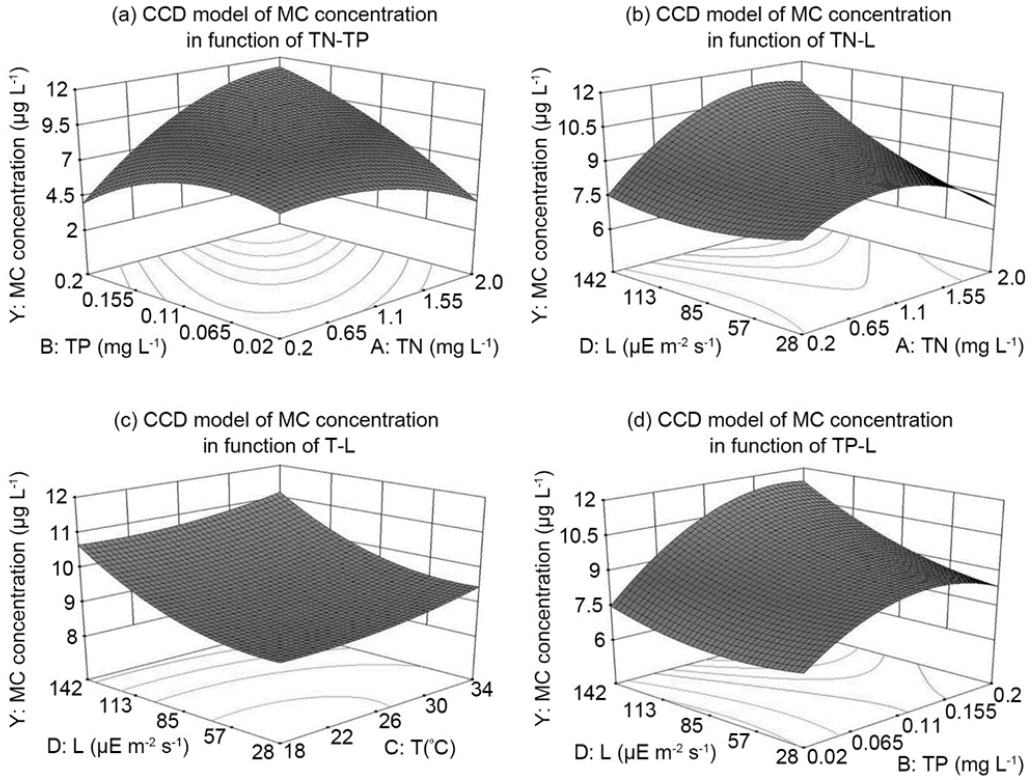

Figure 5. Response surface plots of CCD model of MC concentration. (a) CCD model of MC concentration in function of TN-TP; (b) CCD model of MC concentration in function of TN-L; (c) CCD model of MC concentration in function of T-L; (d) CCD model of MC concentration in function of TP-L.

ceable that MA growth was suppressed with increasing TN concentration under low-light condition (< 90 μE m^{-2} s^{-1}). Figures 4(c) and 4(d) shows the response surface plot as a function of T-L and TP-L, respectively. The maximum MA density was reached at the coded level of +2 for both T-L and TP-L. The promoting effect of temperature on MA growth decreased with increasing light intensity.

3.4. Interactive Effects of Environmental Factors on MC Production

The similar interactive effect of TN and TP (non-linear positive correlation) on MC concentration can be observed in the surface plot in Figure 5(a). The optimum TN/TP ratio for MC production ranged from 9.9 to 10.4, which was slightly higher than that for MA growth. The thresholds of TN and TP concentration that supported the response for MC concentration at 1.0 μg L^{-1} (the provisional safety guideline in potable water recommended by the World Health Organization) ranged between 0.10 ~ 0.37 mg L^{-1} and 0.01 ~ 0.04 mg L^{-1}, respectively. As shown in Figures 5(b) and 5(d), MC production might be restricted upon divergence from the optimum TN/TP ratio when N or P sources was separately raised or reduced. The response surface plot in function of TN-L indicated that the stimulating effect of light intensity on MC production increased with higher TN concentration. Plots in function of TN-L and TP-L suggested that MC concentration gradually declined with increasing MA density at low lights and high nutrients. The promoting effect of light intensity on MC production was greater than that of temperature (Figure 5(c)).

3.5. Validation of CCD Response Surface Models

To confirm the validity of our statistical and experimental strategies, verification experiments were conducted under different culture conditions with environmental variables set close to their seasonal levels in Changtan Reservoir. CCD modeling results were compared with the measured values of MA density and MC concentration in Changtan Reservoir. As shown in Figures 6(a) and 6(b), the verification experimental results in NEBs and the CCD model prediction are generally consistent with the field observations in Changtan Reservoir (standard error < 10%, R-squared > 85%). Model verification was also performed using two other cases of algal blooming formation reported in Taihu Lake of China (Chen et al., 2009) and Vancouver Lake of USA (Lee et al., 2015), which both are typical shallow eutrophic freshwater lakes in the subtropical and temperate zone, respectively (Figures 6(c) and 6(d)). The verification experiments confirmed the critical influence of these environmental factors on MA growth and MC production in natural phytoplankton community. The predicted MA density and MC concentration from the CCD polynomial models were in agreement with the actual values reported from previous studies (standard error < 10%, R-squared > 80%).

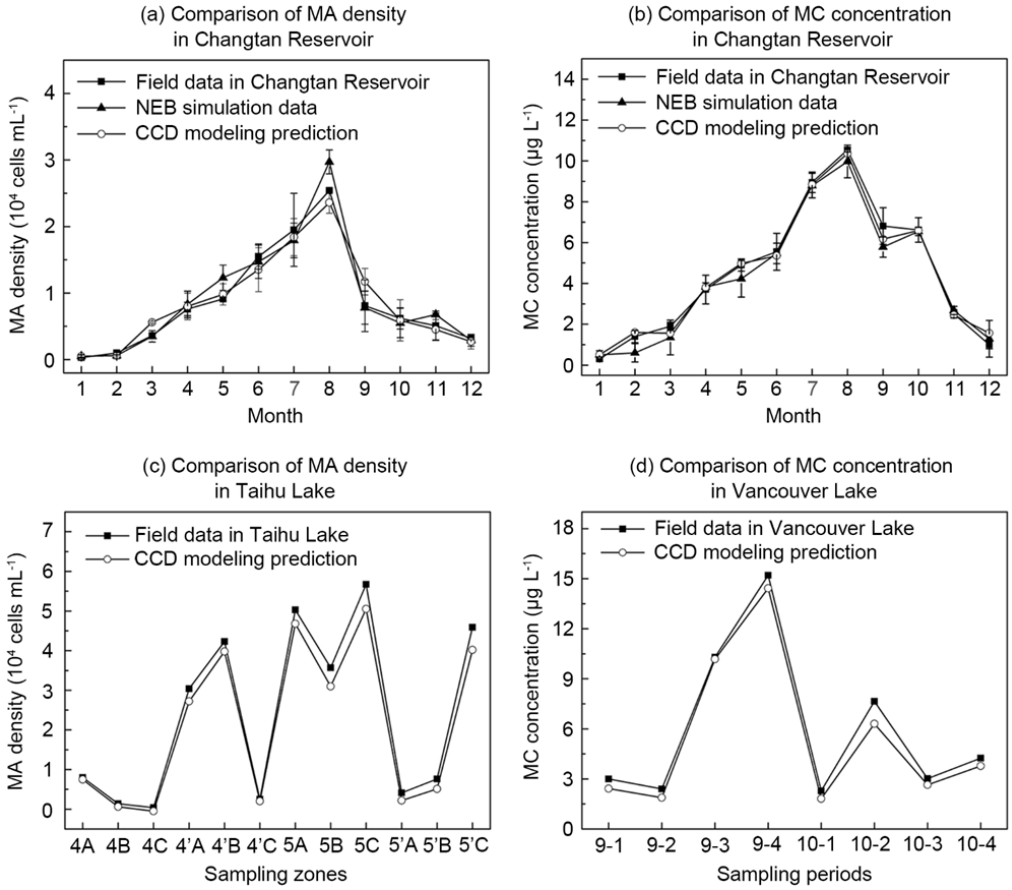

Figure 6. Comparison of predicted data in CCD modeling, experimental data in NEBs, and measured values in natural water bodies. (a) MA density in Changtan Reservoir; (b) MC concentration in Changtan Reservoir; (c) MA density in Taihu Lake; (d) MC concentration in Vancouver Lake.

4. Discussion

4.1. Nutrient Thresholds for Microcystis Blooms and Microcystin Safety

MA dominated the phytoplankton communities in the NEBs and claimed responsibility for the potential blooming formation. As suggested by our PB-designed screening experiments and CCD regression model, the most essential promoting parameters that are associated with the massive proliferation of MA are the interactive effect of both N and P. If N or P was individually overloaded, MA growth might be significantly inhibited as a result of deviation from the optimal TN/TP ratio, which has been collaterally proven by Xie et al. (2003). The significant role of nitrate and phosphate as essential macronutrients influencing the growth, chemical composition and dominance of MA has been widely accepted (Horst et al., 2014). Some earlier arguments asserted that cyanobacterial bloom was more affected by increases in phosphorus rather than simply by a decrease in the N/P ratio (Havens and Walker Jr, 2002). However, recent studies have shown that the stimulating effect of P is related to N and that the occurrence of MA bloom was positively correlated to concentration of both N and P (Kim et al., 2007; Paerl et al., 2011).

Our CCD graphical optimization suggested the nutrient thresholds for the potential MA blooms were TN of 0.20 ~ 0.89 mg L^{-1} and TP of 0.02 ~ 0.08 mg L^{-1}, respectively. The critical values identified in this study were slightly higher than the TN and TP concentration thresholds limiting intrinsic growth rates of MA dominated blooms determined through *in-situ* microcosm nutrient dilution bioassays and mesocosm nutrient addition experiments, which were TN of 0.80 mg L^{-1} and TP of 0.05 mg L^{-1} (Xu et al., 2015). Hai et al. (2010) proposed the nutrient thresholds for the blooming formation of dominant toxin-producing MA through field sampling and *in-situ* nutrient enrichment bioassays, which were TN of 0.80 mg L^{-1} and TP of 0.20 mg L^{-1}. By analyzing long-term data in over 2000 Finnish lakes, Vuorio et al. (2020) identified that TP threshold for MA growth was 0.02 mg L^{-1}. Shan et al. (2020) estimated the lake-specific nutrient thresholds and identified a TP threshold of 0.05 ~ 0.10 mg L^{-1} suppressing total *Microcystis* biomass. Compared to the critical border values stimulating the rapid growth of MA and MC production (TN of 17.78 mg L^{-1} and TP of 3.10 mg L^{-1}) obtained from monoculture experiments (Jiang et al., 2008), our thresholds appeared closer to the field observations.

Our CCD model also identified that TN and TP thresholds for the safety guideline of MC concentration (1.0 μg L^{-1})

ranged between 0.10 ~ 0.37 mg L^{-1} and 0.01 ~ 0.04 mg L^{-1}, respectively. Our study supported the hypothesis that MC concentrations increased with lake trophic status (Kotak et al., 2000) and nutrient thresholds could be stricter by the increase of temperature (Shan et al., 2020). Orihel et al. (2012) reported that the nitrogen and phosphorus thresholds for MC concentration of 1.0 μg L^{-1} in 95% Canadian lakes were 0.658 mg L^{-1} and 0.026 mg L^{-1}, respectively. Kelly et al. (2019) demonstrated that TP concentrations associated with exceedance of drinking water standard for MC concentration was 0.025 mg L^{-1}. Shan et al. (2020) detected a TN threshold of 0.8 mg L^{-1} and TP threshold of 0.05 mg L^{-1} in three eutrophic lakes to maintain MC concentrations below 1.0 μg L^{-1} and found that the effect can be counteracted by the increase of temperature. In this study, we proposed dynamic threshold values of TN and TP in controlling MC risks under lake-dependant conditions of temperature and light intensity, which were generally in consistent with previous studies.

4.2. Interactive Effects of Nitrogen and Phosphorus on Microcystis Growth and Microcystin Production

Our study regulated the concentrations of N and P within a specific range with different N/P ratios, simulating the average nutrient levels of Changtan Reservoir through NEBs. The fittest TN/TP ratio favoring MA growth under different temperatures and light intensities was 9.5 ~ 10.2. Although Downing et al. (2001) stated the possibility that cyanobacterial bloom was more strongly correlated with simple increases in nutrient concentration rather than with the TN/TP ratio, the significant influence of a TN/TP ratio lower than 30 on cyano-bacterial dominance and MA-dominant blooms in the hypertrophic reservoir system has been proposed (Klausmeier et al., 2004; Ptacnik et al., 2010; Liu et al., 2011). The bloom-forming MA was observed to become a superior competitor with a N/P supply ratio lower than 10 in warm temperatures (Kim et al., 2007; Liu et al., 2011). It has been widely reported that N-fixing species had a higher optimum TN/TP ratio than non-N-fixing species because N-fixers need to power N fixation at the expense of P-rich assembly machinery (Klausmeier et al., 2004). The relative abundance of non-N-fixing species (*Microcystis*, *Scenedesmus*, *Melosira*, *Oscillatoria*, etc.) to total algae at different TN/TP ratios was generally greater than 90%, while N-fixing species (*Anabaena*, *Aphanizomenon*, etc.) presented an insignificant fraction of total biomass in the present study. The range of the optimal TN/TP ratio linked to the prediction of MA-dominant blooms suggested by our study was consistent with the above consensus.

The hypothesis that N availability influenced the cyanobacterial composition was supported. Different taxa might respond to the concentration of different N-species in different ways during the process of resource competition, but the uptake of both organic and inorganic species of N in MA appeared to be more efficient than other algae (Paerl et al., 2011). It is known that phytoplankton community rely mainly on DIN in most aquatic systems, but DON constitutes a large pool of fixed N and enhances cyanobacterial development (Monchamp et al., 2014). The DON pool was composed of refractory N-containing compounds, which could be assimilated by toxin-producing taxa such as MA at relatively low cost (Chang et al., 2005). Field investigations and laboratory experiments showed that MC-producing strains yielded higher growth rates than non-MC-producing strains at high concentrations of inorganic N (O'Neil et al., 2012; Singh et al., 2015), which was confirmed by our modeling results. With more inorganic nutrients loaded into freshwater systems, the dominance of the toxic genotype increased and led to a faster competitive exclusion of the non-toxic genotype (Suominen et al., 2016), while toxic MA might outgrow non-toxic MA and synthesis more MCs (Conradie and Barnard, 2012).

4.3. Interactive Effects of Temperature and Light Intensity on Microcystis Growth and Microcystin Production

Light intensity and its interaction with nitrogen were accepted as significant factors for MA growth and MC production in this study. The population of MA tended to increase with enhanced nitrogen content in both high light and low light. MA is a typical low-light-adapted cyanobacterial genus and has competitive advantage over other phytoplankton species at limited light conditions (Yang and Jin, 2008; Domingues et al., 2011). Previous studies have demonstrated that high light conditions could accelerate photosynthesis and stimulate the MA dominance in the community (Havens et al., 1998; Tan et al., 2009). The significant interaction between light intensity and nitrogen concentration on the soluble extracellular polysaccharide content and buoyancy ability has been reported (Brookes and Ganf, 2001; Wang et al., 2011). The MA proportion of all cyanobacteria was strongly linked to MC concentrations (Rinta-Kanto et al., 2009). MC production was found to be enhanced with comparably high MA dominance when environmental nitrogen level and nitrogen uptake rate were higher than that required for balanced growth of MA, supporting the potential role of both N and species composition in influencing bloom toxicity (Monchamp et al., 2014). However, non-toxic strains of MA were better competitors for light resources than toxic strains during the development of dense MA blooms (Kardinaal et al., 2007), offering a plausible explanation for the gradual decrease in average cellular toxicity.

CCD modeling results indicated that temperature was less associated with MA growth and MC production than was illumination. Temperature was considered as one of the most significant observable effects of global warming in enhancing the risk of MA blooms with respect to N/P ratio (Liu et al., 2011). The effect of a suitable temperature on the growth and polysaccharide content of MA depended on light intensity (Cao et al., 2011; Domingues et al., 2011). MA abundance was observed with a notable increase under low light when water temperature was high, with the dominance of all other light-favoring genera fading. As a low-light-energy-requiring genus, MA has a greater ability than other cyanobacterial taxa to endure the stress of darkness and low temperature, contributing a larger proportion toward the total phytoplankton growth (O'Neil et al., 2012).

MA was therefore assumed to gain a constant advantage in phytoplankton succession due to its tolerance and susceptibility in various environmental conditions. Higher temperature not only promoted MA blooms but also favored the proliferation of MC-producing strains in the community. The elevated temperature yielded more toxic MA cells with MC synthetase gene operons, leading to an active promotion of MC content (Davis et al., 2009).

4.4. Limitation and Future Improvements

Previous studies were mostly conducted with MA single isolates in the basic form of nutrient enrichment bioassays under artificially static culture conditions. However, the impact of hydrologic disturbance on phytoplankton productivity and competition has been ignored in these experiments. Meanwhile, the commonly used approaches of statistical modelling have not fully captured the complex response of cyanobacterial biomass and microcystin concentration in relation to the stochastic variation of ambient conditions. Our study simulated the hydrodynamic condition of real aquatic environments by applying the pneumatic annular flume microcosm system to investigate MA growth and MC production in the context of natural phytoplankton succession. The response surface modelling methodology employed to predict the interactive effects of environmental factors on growth and MC production of MA strain in the natural phytoplankton community was validated by field data. However, it should be noted that the environmental conditions of natural lake and reservoir are quite different from those in validation experiments. Real-world aquatic system differs in many aspects including nutrients, temperature range, cyanobacterial community, succession patterns (Kelly et al., 2019). Prediction strategies for cyanobacterial growth and cyanotoxins were largely dependent on lake-specific environmental gradients (Taranu et al., 2017). Although the predicted values of our second-order polynomial models for MA density and MC content fit well with the experimental results and previously reported field data, the uncertainty of the predictive regression models suggested that our statistical simulation should be treated with caution. Prediction of variation in MA growth and MC production should require a broader knowledge of environmental conditions for the establishment of proposed models. In future, the repetition of this modelling process in other blooming lake or reservoir might be preferable to the indiscriminate use of models, and some other meteorological or hydrologic factors might be determining to improve the predictive performance. Further research is also required to investigate the response of potential toxic effect of other cyanotoxins under the interactive effect of environmental factors.

5. Conclusion

Unlike previous studies conducting NEBs with single MA isolates under artificially static culture conditions, this study performed a batch of ambient-controlled NEBs by applying statistically based experimental design, and simulated the hydrodynamic condition of real aquatic environments by applying the pneumatic annular flume microcosm system to investigate MA growth and MC production in the context of natural phytoplankton succession. Instead of adopting one-at-a-time method, a second-order polynomial response surface model was established to evaluate the interactive effects of TN, TP, T, and L on MA growth and MC production in the natural phytoplankton community. The interactive effects of TN-TP and TN-L on both MA density and MC concentration were determined to be more significant than other factors. The range of the optimum TN/TP ratio for MA growth and MC production under different temperature and light intensities was 9.5 ~ 10.2 and 9.9 ~ 10.4, respectively. The dynamic nutrient thresholds that supported the minimum MA density of 2.00×10^4 cells mL^{-1} (potential criteria of MA bloom event) were determined as TN of 0.20 ~ 0.89 mg L^{-1} and TP of 0.02 ~ 0.08 mg L^{-1}. The thresholds supporting the criteria for MC concentration of 1.0 μg L^{-1} were determined as TN of 0.10 ~ 0.37 mg L^{-1} and TP of 0.01 ~ 0.04 mg L^{-1}. Our study implied that the effects of nitrogen and phosphorus on MA growth and MC production were associated with temperature and light intensity, and the nutrient thresholds for MA blooming events and cyanotoxins safety guideline were fluctuant under lake-dependant conditions of temperature and light intensity. Moreover, the optimum TN/TP mass ratios should be alerted for the eutrophication management of blooming formation and microcystin safety. These results constituted valuable insights on MA dynamics and MC production, triggering events which can be applied to predict the response of such cyanobacterial strains to variations occurring in aquatic environments.

Acknowledgements. This work was funded by the Key Program of NSFC (91647206), the National Science Funds for Creative Research Groups of China (51421006), NSFC (52070132), YESS by CAST (2018QNRC001), the Outstanding Youth Fund of Jiangsu Province (BK20200053) and PAPD.

References

Beuckels, A., Smolders, E. and Muylaert, K. (2015). Nitrogen availability influences phosphorus removal in microalgae-based wastewater treatment. *Water Res.*, 77, 98-106. https://doi.org/10.1016/j.watres.2015.03.018

Bouhaddada, R., Nélieu, S., Nasri, H., Delarue, G. and Bouaïcha, N. (2016). High diversity of microcystins in a Microcystis bloom from an Algerian lake. *Environ. Pollut*., 216, 836. https://doi.org/10.1016/j.envpol.2016.06.055

Brookes, J.D. and Ganf, G.G. (2001). Variations in the buoyancy response of Microcystis aeruginosa to nitrogen, phosphorus and light. *J. Plankton. Res.*, 23(12), 1399-1411. https://doi.org/10.1093/plankt/23.12.1399

Buyukates,Y. and Roelke, D. (2005). Influence of pulsed inflows and nutrient loading on zooplankton and phytoplankton community structure and biomass in microcosm experiments using estuarine assemblages. *Hydrobiologia*, 548(1), 233-249. https://doi.org/10.1007/s10750-005-5195-x

Cao, C., Zheng, B., Chen, Z., Huang, M. and Zhang, J. (2011). Eutrophication and algal blooms in channel type reservoirs: A novel enclosure experiment by changing light intensity. *Res. J. Environ. Sci*., 23(10), 1660-1670. https://doi.org/10.1016/S1001-0742(10)60587-6

Flores, E. and Herrero, A. (2005). Nitrogen assimilation and nitrogen

control in Cyanobacteria. *Biochem. Soc. Trans*., 33(1), 164-167. https://doi.org/10.1042/BST0330164

Chen, F.Z., Song, X.L., Hu, Y.H., Liu, Z.W. and Qin, B.Q. (2009). Water quality improvement and phytoplankton response in the drinking water source in Meiliang Bay of Lake Taihu, China. *Ecol. Eng*., 35(11), 1637-1645. https://doi.org/10.1016/j.ecoleng.2008.01.001

Conradie, K.R. and Barnard, S. (2012). The dynamics of toxic Microcystis strains and microcystin production in two hypertrofic South African reservoirs. *Harmful Algae*, 20(14), 1-10. https://doi.org/10.1016/j.hal.2012.03.006

Daly, R.I., Ho, L. and Brookes, J.D. (2007). Effect of chlorination on Microcystis aeruginosa cell integrity and subsequent microcystin release and degradation. *Environ. Sci. Technol.*, 41(12), 4447- 4453. https://doi.org/10.1021/es070318s

Davis, T.W., Berry, D.L., Boyer, G.L. and Gobler, C.J. (2009). The effects of temperature and nutrients on the growth and dynamics of toxic and non-toxic strains of Microcystis during cyanobacteria blooms. *Harmful Algae*, 8(5), 715-725. https://doi.org/10.1016/j.hal.2009.02.004

Dolman, A.M., Rücker, J., Pick, F.R., Fastner, J., Rohrlack, T., Mischke, U. and Wiedner, C. (2012). Cyanobacteria and cyanotoxins: The influence of nitrogen versus phosphorus. *Plos One*, 7(6), e38757. https://doi.org/10.1371/journal.pone.0038757

Domingues, R.B., Anselmo, T.P., Barbosa, A.B., Sommer, U. and Galvão, H.M. (2011). Light as a driver of phytoplankton growth and production in the freshwater tidal zone of a turbid estuary. *Estuar. Coast. Shelf Sci*., 91(4), 526-535. https://doi.org/10.1016/j.ecss.2010.12.008

Domingues, R.B., Barbosa, A.B., Sommer, U. and Galvao, H.M. (2012). Phytoplankton composition, growth and production in the Guadiana estuary (SW Iberia): Unraveling changes induced after dam construction. *Sci. Total Environ*., 416, 300-313. https://doi.org/10.1016/j.scitotenv.2011.11.043

Donald, D.B., Bogard, M.J., Finlay, K., Bunting, L. and Leavitt, P.R. (2013). Phytoplankton-specific response to enrichment of phosphorus-rich surface waters with ammonium, nitrate, and urea. *Plos One*, 8(1), e53277. https://doi.org/10.1371/journal.pone.0053277

Downing, J.A., Watson, S.B. and McCauley, E. (2001). Predicting cyanobacteria dominance in lakes. *Can. J. Fish Aquat. Sci.*, 58 (10), 1905-1908. https://doi.org/10.1139/f01-143

Elliott, J.A. (2012). Predicting the impact of changing nutrient load and temperature on the phytoplankton of England's largest lake, Windermere. *Freshw. Biol.*, 57(2), 400-413. https://doi.org/10.1111/j.1365-2427.2011.02717.x

Garg, M.C. and Joshi, H. (2017). Comparative assessment and multivariate optimization of commercially available small scale reverse osmosis membranes. *J. Environ. Inform*., 29(1), 39-52. https://doi.org/10.3808/jei.201700357

Geada,P., Pereira,R.N.,Vasconcelos, V., Vicente, A.A. and Fernandes, B.D. (2017). Assessment of synergistic interactions between environmental factors on Microcystis aeruginosa growth and microcystin production. *Algal Res*., 27, 235-243. https://doi.org/10.1016/j.algal.2017.09.006

Genuário, D.B., Lorenzi, A.S., Agujaro, L.F., Isaac, R.D.L., Azevedo, M.T.D.P., Neto, R.C. and Fiore, M.F. (2016). Cyanobacterial community and microcystin production in a recreational reservoir with constant Microcystis blooms. *Hydrobiologia*, 779(1), 105-125. https://doi.org/10.1007/s10750-016-2802-y

Xu, H., Paerl, H.W., Qin, B.Q., Zhu, G.W. and Gao, G.A. (2010). Nitrogen and phosphorus inputs control phytoplankton growth in eutrophic Lake Taihu, China. *Limnol. Oceanogr*., 55(1), 420-432. https://doi.org/10.4319/lo.2010.55.1.0420

Hanrahan, G., Garza C., Garcia1 E. and Miller K. (2007). Experimental design and response surface modeling: A method development application for the determination of reduced inorganic species in environmental samples. *J. Environ. Inform*., 9(2), 71-79. https://doi. org/10.3808/jei.200700088

Havens, K.E., Phlips, E.J., Cichra, M.F. and Li, B.L. (1998). Light availability as a possible regulator of cyanobacteria species composition in a shallow subtropical lake. *Freshw. Biol*., 39(3), 547-556. https://doi.org/10.1046/j.1365-2427.1998.00308.x

Havens, K.E. and Walker Jr, W.W. (2002). Development of a total phosphorus concentration goal in the TMDL process for Lake Okeechobee, Florida (USA). *Lake Reservoir Manag*., 18(3), 227-238. https://doi.org/10.1080/07438140209354151

Horst, G.P., Sarnelle, O., White, J.D., Hamilton, S.K., Kaul, R.R.B. and Bressie, J.D. (2014). Nitrogen availability increases the toxin quota of a harmful cyanobacterium, Microcystis aeruginosa. *Water Res.*, 54(4), 188-198. https://doi.org/10.1016/j.watres.2014.01.063

Hu, H.J. and Wei Y.X. (2006). *The freshwater algae of China: Systematics, taxonomy and ecology*. Science Press, Beijing, China.

Huang, W., Zhu, X., Zeng, J., He, Q., Xu, X., Liu, J., Jiang, Z., Dou, S. and Chen, Q. (2012). Responses in growth and succession of the phytoplankton community to different N/P ratios near Dongtou Island in the East China Sea. *J. Exp. Mar. Biol. Ecol*., 434, 102-109. https://doi.org/10.1016/j.jembe.2012.08.008

Jiang, Y., Ji, B., Wong, R.N.S. and Wong, M.H. (2008). Statistical study on the effects of environmental factors on the growth and microcystins production of bloom-forming cyanobacterium—Microcystis aeruginosa. *Harmful Algae*, 7(2), 127-136. https://doi.org/10.1016/j.hal.2007.05.012

Kardinaal, W.E.A., Tonk, L., Janse, I., Hol, S., Slot, P., Huisman, J., Visser, P.M. (2007). Competition for light between toxic and nontoxic strains of the harmful cyanobacterium Microcystis. *Appl. Environ. Microbiol*., 73(9), 2939. https://doi.org/10.1128/AEM.02892-06

Kelly, N.E., Javed, A., Shimoda, Y., Zastepa, A., Watson, S., Mugalingam, S. and Arhonditsis, G.B. (2019). A Bayesian risk assessment framework for microcystin violations of drinking water and recreational standards in the Bay of Quinte, Lake Ontario, Canada. *Water Res*., 162, 288-301. https://doi.org/10.1016/j.watre s.2019.06.005

Kim, H.S., Hwang, S.J., Shin, J.K., An, K.G. and Yoon, C.G. (2007). Effects of limiting nutrients and N:P ratios on the phytoplankton growth in a shallow hypertrophic reservoir. *Hydrobiologia*, 581 (1), 255-267. https://doi.org/10.1007/s10750-006-0501-9

Klausmeier, C.A., Litchman, E., Daufresne, T. and Levin, S.A. (2004). Optimal nitrogen-to-phosphorus stoichiometry of phytoplankton. *Nature*, 429(6988), 171-174. https://doi.org/10.1038/natur e02454

Kong, Y., Zou, P., Miao, L., Qi, J., Song, L., Zhu, L. and Xu, X. (2014). Medium optimization for the production of anti-cyanobacterial substances by Streptomyces sp. HJC-D1 using response surface methodology. *Environ. Sci. Pollut. Res*., 21, 5983-5990. https://doi.org/10.1007/s11356-014-2532-5

Kotak, B.G., Lam, A.K.Y., Prepas, E.E. and Hrudey, S.E. (2000). Role of chemical and physical variables in regulating microcystin- LR concentration in phytoplankton of eutrophic lakes. *Can. J. Fish Aquat. Sci*., 57(8), 1584-1593. https://doi.org/10.1139/f00-091

Lee, T.A., Rollwagen-Bollens, G., Bollens, S.M. and Faber-Hammond, J.J. (2015). Environmental influence on cyanobacteria abundance and microcystin toxin production in a shallow temperate lake. *Ecotoxicol. Environ. Saf*., 114, 318-325. https://doi.org/10.1016/j.ecoenv.2014.05.004

Lei, L., Li, C., Peng, L. and Han, B.P. (2015). Competition between toxic and non-toxic Microcystis aeruginosa and its ecological implication. *Ecotoxicology*, 24(7-8), 1411-1418. https://doi.org/10.1007/s10646-015-1456-2

Liu, X., Lu, X. and Chen, Y. (2011). The effects of temperature and nutrient ratios on Microcystis blooms in Lake Taihu, China: An 11-year investigation. *Harmful Algae*, 10(3), 337-343. https://doi.org/10.1016/j.hal.2010.12.002

Lucker, B.F., Hall, C.C., Zegarac, R. and Kramer, D.M. (2014). The

environmental photobioreactor (ePBR): An algal culturing platform for simulating dynamic natural environments. *Algal Res*., 6, 242-249. https://doi.org/10.1016/j.algal.2013.12.007

Monchamp, M.E., Pick, F.R., Beisner, B.E. and Maranger, R. (2014). Nitrogen forms influence microcystin concentration and composition via changes in cyanobacterial community structure. *Plos One*, 9(1), e85573. https://doi.org/10.1371/journal.pone.0085573

Narwani, A., Bentlage, B., Alexandrou, M.A., Fritschie, K.J., Delwiche, C., Oakley, T.H. and Cardinale, B.J. (2017). Ecological interactions and coexistence are predicted by gene expression similarity in freshwater green algae. *J. Eco*., 105(3), 580-591. https://doi.org/10.1111/1365-2745.12759

O'Neil, J.M., Davis, T.W., Burford, M.A. and Gobler, C.J. (2012). The rise of harmful cyanobacteria blooms: The potential roles of eutrophication and climate change. *Harmful Algae*. 14(1), 313-334. https://doi.org/10.1016/j.hal.2011.10.027

Orihel, D.M., Bird, D.F., Brylinsky, M., Chen, H., Donald, D.B., Huang, D.Y., Giani, A., Kinniburgh, D., Kling, H., Kotak, B.G., Leavitt, P.R., Nielsen, C.C., Reedyk, S., Rooney, R.C., Watson, S.B., Zurawell, R.W. and Vinebrooke, R.D. (2012). High microcystin concentrations occur only at low nitrogen-to-phosphorus ratios in nutrient-rich Canadian lakes. *Can. J. Fish. Aquat. Sci*., 69(9), 1457-1462. https://doi.org/10.1139/F2012-088

Otten, T.G., Xu, H., Qin, B., Zhu, G. and Paerl, H.W. (2012). Spatio-temporal patterns and ecophysiology of toxigenic Microcystis blooms in Lake Taihu, China: Implications for water quality management. *Environ. Sci. Technol*., 46(6), 3480. https://doi.org/10.1021/es2041288

Paerl, H.W., Xu, H., McCarthy, M.J., Zhu, G.W., Qin, B.Q., Li, Y.P. and Gardner, W.S. (2011). Controlling harmful cyanobacterial blooms in a hyper-eutrophic lake (Lake Taihu, China): The need for a dual nutrient (N & P) management strategy. *Water Res*., 45 (5), 1973-1983. https://doi.org/10.1016/j.watres.2010.09.018

Pimentel, J.S. and Giani, A. (2014). Microcystin production and regulation under nutrient stress conditions in toxic Microcystis strains. *Appl. Environ. Microbiol*., 80(18), 5836-5843. https://doi.org/10.1128/AEM.01009-14

Ptacnik, R., Andersen, T. and Tamminen, T. (2010). Performance of the Redfield ratio and a family of nutrient limitation indicators as thresholds for phytoplankton N vs. P limitation. *Ecosystems*, 13(8), 1201-1214. https://doi.org/10.1007/s10021-010-9380-z

Rinta-Kanto, J.M., Konopko, E.A., Debruyn, J.M., Bourbonniere, R.A., Boyer, G.L. and Wilhelm, S.W. (2009). Lake Erie Microcystis: Relationship between microcystin production, dynamics of genotypes and environmental parameters in a large lake. *Harmful Algae*, 8(5), 665-673. https://doi.org/10.1016/j.hal.2008.12.004

Shan, K., Wang, X.X., Yang, H., Zhou, B.T., Song, L.R. and Shang, M.S. (2020). Use statistical machine learning to detect nutrient thresholds in Microcystis blooms and microcystin management. *Harmful Algae*. 94, 101807. https://doi.org/10.1016/j.hal.2020.101807

Singh, S., Rai, P.K., Chau, R., Ravi, A.K., Neilan, B.A. and Asthana, R.K. (2015). Temporal variations in microcystin-producing cells and microcystin concentrations in two fresh water ponds. *Water Res*., 69, 131-142. https://doi.org/10.1016/j.watres.2014.11.015

Steffen, M.M., Davis, T.W., McKay, R.M.L., Bullerjahn, G.S., Krausfeldt, L.E., Stough, J.M.A., Neitzey, M.L., Gilbert, N.E., Boyer, G.L., Johengen, T.H., Gossiaux, D.C., Burtner, A.M., Palladino, D., Rowe, M.D., Dick, G.J., Meyer, K.A., Levy, S., Boone, B.E., Stumpf, R.P., Wynne, T.T., Zimba, P.V., Gutierrez, D., Wilhelm, S.W. (2017). Ecophysiological examination of the Lake Erie Microcystis bloom in 2014: linkages between biology and the water supply shutdown of Toledo, Ohio. *Environ. Sci. Technol*., 51(12). https://doi.org/10.1021/acs.est.7b00856

Su, J., Yang, X., Zheng, T. and Hong, H. (2007). An efficient method to obtain axenic cultures of Alexandrium tamarense—a PSP-producing dinoflagellate. *J. Microbiol. Methods*., 69(3), 425-430. https://doi.org/10.1016/j.mimet.2006.07.005

Suominen, S., Brauer, V.S., Rantala-Ylinen, A., Sivonen, K. and Hiltunen, T. (2016). Competition between a toxic and a non-toxic Microcystis strain under constant and pulsed nitrogen and phosphorus supply. *Aquat. Ecol*., 51, 117-130. https://doi.org/10.1007/s10452-016-9603-2

Tan, X., Kong, F.X., Zeng, Q.F., Cao, H.S., Qian, S.Q. and Zhang, M. (2009). Seasonal variation of Microcystis in Lake Taihu and its relationships with environmental factors. *J. Environ. Sci-China*, 21(7), 892-899. https://doi.org/10.1016/S1001-0742(08)62359-1

Taranu, Z.E., Gregory-Eaves, I., Steele, R.J., Beaulieu, M. and Legendre, P. (2017). Predicting microcystin concentrations in lakes and reservoirs at a continental scale: A new framework for modelling an important health risk factor. *Glob. Ecol. Biogeogr.*, 26(6), 625-637. https://doi.org/10.1111/geb.12569

Torres, C.D.A., Lürling, M. and Marinho, M.M. (2016). Assessment of the effects of light availability on growth and competition between strains of Planktothrix agardhii and Microcystis aerugino- sa. *Microb Ecol*., 71(4), 802-813. https://doi.org/10.1007/s00248-0 15-0719-z

Vuorio, K.,Järvinen, M. and Kotamäki, N. (2020). Phosphorus thresholds for bloom-forming cyanobacterial taxa in boreal lakes. *Hydrobiologia*, 847(21), 4389-4400. https://doi.org/10.1007/s10750-019-04161-5

Wang, C., Wang, Z., Wang, P. and Zhang, S. (2016). Multiple effects of environmental factors on algal growth and nutrient thresholds for harmful algal blooms: Application of response surface methodology. *Environ. Model. Assess*., 21(2), 247-259. https://doi.org/10.1007/s10666-015-9481-3

Wang, F., Wang, X., Zhao, Y., Yang, F. (2015). Long-term water quality variations and chlorophyll a aimulation with an emphasis on different hydrological periods in Lake Baiyangdian, Northern China. *J. Environ. Inform*., 20(2), 90-102. https://doi.org/10.3808/jei.201200223

Wang, W., Liu, Y., Geng, L., Yang, Z. and Chen, Y. (2011). The effect of nitrogen concentration and its interaction with light intensity on population dynamics and polysaccharide content of Microcystis aeruginosa. *J. Freshw. Ecol*., 26(2), 241-248. https://doi.org/10.1080/02705060.2011.555205

Wang, Z., Chen, Q., Hu, L. and Wang, M. (2017). Combined effects of binary antibiotic mixture on growth, microcystin production, and extracellular release of Microcystis aeruginosa: application of response surface methodology. *Environ. Sci. Pollut. Res*., 25, 736-748. https://doi.org/10.1007/s11356-017-0475-3

Zhu, W., Zhou, X., Chen, H., Gao, L., Xiao, M. and Li, M. (2016). High nutrient concentration and temperature alleviated formation of large colonies of Microcystis: Evidence from field investigations and laboratory experiments. *Water Res*., 101, 167-175. https://doi.org/10.1016/j.watres.2016.05.080

Xie, L., Xie, P., Li, S., Tang, H. and Liu, H. (2003). The low TN:TP ratio, a cause or a result of Microcystis blooms? *Water Res*., 37(9), 2073-2080. https://doi.org/10.1016/S0043-1354(02)00532-8

Xu, H., Paerl, H.W., Qin, B., Zhu, G., Hall, N.S. and Wu, Y. (2015). Determining critical nutrient thresholds needed to control harmful cyanobacterial blooms in eutrophic Lake Taihu, China. *Environ. Sci. Technol*., 49(2), 1051-1059. https://doi.org/10.1021/es503744q

Yang, S. and Jin, X. (2008). Critical light intensities for Microcystis aeruginosa, Scenedesmus quadricauda and Cyclotella sp. and competitive growth patterns under different light:N:P ratios. *J. Freshw. Ecol*., 23(3), 387-396. https://doi.org/10.1080/02705060.2008.9664215

Yang, Z., Geng, L., Wang, W. and Zhang, J. (2012). Combined effects of temperature, light intensity, and nitrogen concentration on the growth and polysaccharide content of Microcystis aeruginosa in

batch culture. *Biochem. Syst. Ecol*., 41(1), 130-135. https://doi.org/10.1016/j.bse.2011.12.015

Yu, L., Kong, F., Zhang, M., Yang, Z., Shi, X. and Du, M. (2014). The dynamics of microcystis genotypes and microcystin produc- tion and associations with environmental factors during blooms in Lake Chaohu, China. *Toxins*, 6(12), 3238-3257. https://doi.org/10.3390/toxins6123238

Zhang, M., Qin, B.L., Yu, Y., Yang, Z., Shi, X.L. and Kong, F.X. (2016). Effects of temperature fluctuation on the development of cyanobacterial dominance in spring: implication of future climate change. *Hydrobiologia*, 763(1), 135-146. https://doi.org/10.1007/s10750-015-2368-0

Zheng, S., Wang, P., Wang, C., Hou, J. and Qian, J. (2013). Distribution of metals in water and suspended particulate matter during the resuspension processes in Taihu Lake sediment, China. *Quat. Int*., 286(3), 94-102. https://doi.org/10.1016/j.quaint.2012.09.003

Zhu, X., Wang, J., Lu, Y., Chen, Q. and Yang, Z. (2015). Grazer-induced morphological defense in Scenedesmus obliquus is affected by competition against Microcystis aeruginosa. *Sci. Rep*., 5, 12743. https://doi.org/10.1038/srep12743